Research article JHEP|Reports

Direct mechanical exposure initiates hepatocyte proliferation

Authors

Wang Li, Yi Wu, Wenhui Hu, Jin Zhou, Xinyu Shu, Xiaoyu Zhang, Ziliang Zhang, Huan Wu, Yu Du, Dongyuan Lü, Shouqin Lü, Ning Li, Mian Long

Correspondence

mlong@imech.ac.cn (M. Long), lining_1@imech.ac.cn (N. Li).

Graphical abstract

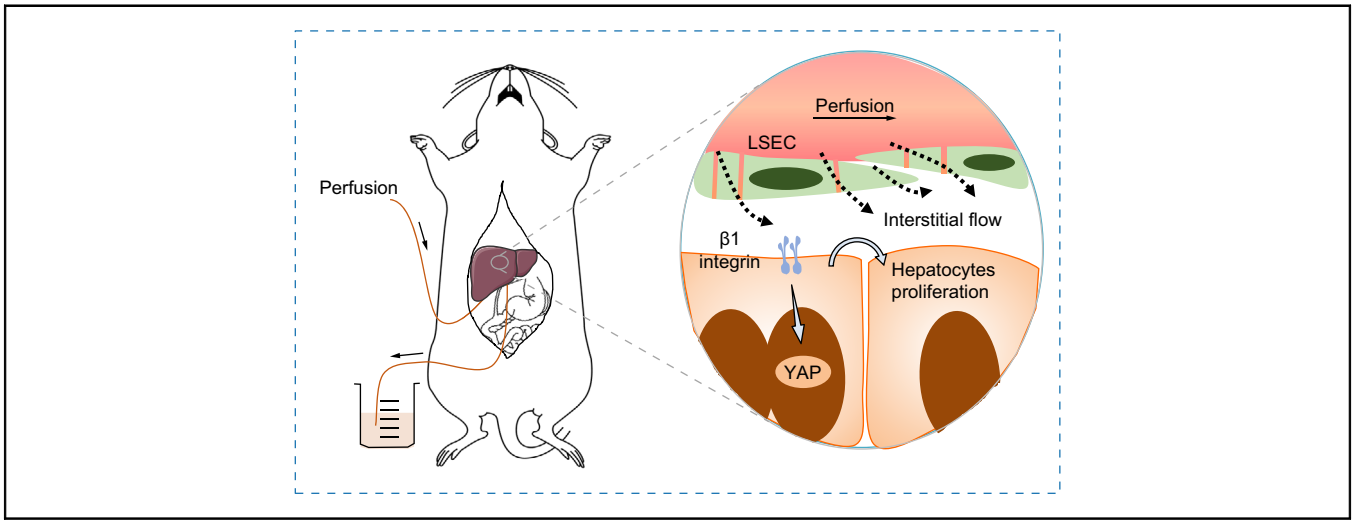

Highlights

- *Ex vivo* liver perfusion stimulates hepatocytes to re-enter the cell cycle.
- Flow-induced shear stress induces hepatocyte proliferation *in vitro.*
- β1 integrin-YAP mechanotransduction is essential for shear-enhanced proliferation.

Impact and implications

By using both *ex vivo* liver perfusion and *in vitro* flow exposure tests, we identified the roles of interstitial flow in the space of Disse in stimulating hepatocytes to re-enter the cell cycle. We found an increase in shear flow-induced hepatocyte proliferation via β1 integrin-YAP mechanotransductive pathways. This serves as a useful model to potentiate hepatocyte expansion *in vitro* using mechanical forces.

https://doi.org/10.1016/j.jhepr.2023.100905

Research article

JHEP|Reports

Direct mechanical exposure initiates hepatocyte proliferation

Wang Li,[1,2] Yi Wu,[1,2] Wenhui Hu,[1] Jin Zhou,[1] Xinyu Shu,[1,2] Xiaoyu Zhang,[1,2] Ziliang Zhang,[1,3] Huan Wu,[1] Yu Du,[1] Dongyuan Lü,[1,2] Shouqin Lü,[1,2] Ning Li,[1,2,*] Mian Long[1,2,*]

[1]*Center for Biomechanics and Bioengineering, Beijing Key Laboratory of Engineered Construction and Mechanobiology and Key Laboratory of Microgravity (National Microgravity Laboratory), Institute of Mechanics, Chinese Academy of Sciences, Beijing, China;* [2]*School of Engineering Sciences, University of Chinese Academy of Sciences, Beijing, China;* [3]*Medical Science and Technology Innovation Center, Shandong First Medical University & Shandong Academy of Medical Sciences, China*

JHEP Reports **2023.** https://doi.org/10.1016/j.jhepr.2023.100905

Background & Aims: Liver paracrine signaling from liver sinusoid endothelial cells to hepatocytes in response to mechanical stimuli is crucial in highly coordinated liver regeneration. Interstitial flow through the fenestrated endothelium inside the space of Disse potentiates the role of direct exposure of hepatocytes to fluid flow in the immediate regenerative responses after partial hepatectomy, but the underlying mechanisms remain unclear.
Methods: Mouse liver perfusion was used to identify the effects of interstitial flow on hepatocyte proliferation *ex vivo*. Isolated hepatocytes were further exposed to varied shear stresses directly *in vitro*. Knockdown and/or inhibition of mechanosensitive proteins were used to unravel the signaling pathways responsible for cell proliferation.
Results: An increased interstitial flow was visualized and hepatocytes' regenerative response was demonstrated experimentally by *ex vivo* perfusion of mouse livers. *In vitro* measurements also showed that fluid flow initiated hepatocyte proliferation in a duration- and amplitude-dependent manner. Mechanistically, flow enhanced β1 integrin expression and nuclear translocation of YAP (yes-associated protein), via the Hippo pathway, to stimulate hepatocytes to re-enter the cell cycle.
Conclusions: Hepatocyte proliferation was initiated after direct exposure to interstitial flow *ex vivo* or shear stress *in vitro*, which provides new insights into the contributions of mechanical forces to liver regeneration.
Impact and implications: By using both *ex vivo* liver perfusion and *in vitro* flow exposure tests, we identified the roles of interstitial flow in the space of Disse in stimulating hepatocytes to re-enter the cell cycle. We found an increase in shear flow-induced hepatocyte proliferation via β1 integrin-YAP mechanotransductive pathways. This serves as a useful model to potentiate hepatocyte expansion *in vitro* using mechanical forces.

Introduction

The liver has an outstanding capacity to regenerate after injury and is able to restore its original weight within 5 to 7 days after two-thirds partial hepatectomy (PHx) in rats.[1] The portal vein flow is increased about threefold immediately after two-thirds PHx, followed by a series of rapid responses, *i.e.*, the activity of urokinase-type plasminogen activator is increased within 1 min, nuclear translocation of β-catenin and Notch intracellular domain takes place within 30 min to initiate regenerative responses, and hepatocyte growth factor (HGF) and epidermal growth factor receptors are activated 1 h later.[2] The regenerative process is delayed when the portal blood flow is decreased by constructing a bypass vessel between the portal vein and inferior vena cava after PHx.[3] Specifically, the hemodynamic changes in the branched blood vessels after PHx are closely related to the subsequent regeneration rate,[4] indicating that there is a correlation between liver tissue regeneration and localized blood flow. Moreover, blood flow is heterogeneously distributed in the remnant branched blood vessels after PHx, resembling the differential distribution of hepatocyte proliferation.[5] These mechanical cues suggest that blood flow-induced mechanical alterations may act as a key trigger for liver regeneration.

As the first cell type exposed to sinusoidal blood flow, liver sinusoidal endothelial cells (LSECs) are subjected to mechanical stretch or shear and secrete HGF or downregulate transforming growth factor β1 (TGF-β1) expression to promote hepatocyte proliferation.[3,6] On the other hand, the interstitial flow in the space of Disse could also be critical since the sinusoidal endothelium is highly permeable, with distributed clusters of fenestrae (diameter ranging from 150 to 200 nm) on LSECs and gaps between LSECs.[7,8] While the effects of interstitial flow on liver regeneration after PHx are often neglected because of the technical difficulty in studying them, it is plausible that hepatocytes underneath the endothelium can also respond to hemodynamic changes in the sinusoids by sensing interstitial flow alterations directly. In fact, hepatocytes are known to be mechanosensitive in many liver-specific functions, which are promoted by low shear stress but impaired by high shear stress.[9] Thus, it is

Keywords: Mechanotransduction; FAK; hepatic sinusoid chip.
Received 18 February 2023; received in revised form 29 August 2023; accepted 31 August 2023; available online 15 September 2023
* Corresponding author. Address: Institute of Mechanics, Chinese Academy of Sciences, Beijing, 100190, China.
E-mail addresses: mlong@imech.ac.cn (M. Long), lining_1@imech.ac.cn (N. Li).

reasonably hypothesized that the interstitial flow might participate in initiating liver regeneration starting from hepatocyte proliferation.

Mechanotransductive pathways are key to sense and respond to mechanically induced cues. For example, yes-associated protein (YAP) is known to promote immortalized epithelial cell proliferation in response to mechanical stimuli, including low cell density, large cell geometry, or stiff substrate.[10] Phosphorylated inactive YAP is retained in the cytosol by binding to 14-3-3, catenin or angiomotin, until upstream stimuli interrupt this binding and release YAP to translocate into the nucleus.[11] One of the key upstream molecules is membranous integrin, together with its cytoplasmic partners such as focal adhesion kinase (FAK), talin, vinculin and paxillin. Meanwhile, activation of the integrin-FAK signaling pathway promotes hepatocellular carcinoma (HCC) proliferation but negatively regulates liver-specific functions in response to increased matrix stiffness.[12,13] On the other hand, β1 integrin and YAP signaling are required for liver regeneration. YAP knockout in hepatocytes significantly attenuates CAR (constitutive androstane receptor)- or SHP2 (tyrosine-protein phosphatase nonreceptor type 11)-mediated proliferation of mouse hepatocytes after PHx,[14,15] while YAP hyperactivation leads to liver overgrowth.[16] Hepatocyte-specific knockout or knockdown of β1 integrin impairs liver regeneration by inhibiting the signaling of related growth factors.[17] These observations suggest that mechanosensitive integrin and YAP are essential for hepatocyte proliferation, but their roles in shear-initiated hepatocyte proliferation are still unknown. Hence, we aimed to determine the role of interstitial flow in the initiation of hepatic regeneration as well as elucidate the underlying mechanotransductive mechanisms.

Materials and methods

Cell culture

6- to 8-week-old C57BL/6N male mice (Vital River Laboratories, Beijing, China) were used for hepatocyte isolation, as previously described.[8] All animal protocols were approved by the Institutional Animal and Medicine Ethical Committee at the Institute of Mechanics of the Chinese Academy of Sciences. Please refer to the supplementary information for more details.

Ex vivo liver perfusion

Liver perfusion was performed by a modified procedure described previously.[6] Briefly, the mouse was anesthetized by pentobarbital sodium injection before the portal vein was cannulated with a 24 G intravenous catheter connected to a perfusion system. The perfused Krebs–Henseleit saline solution was oxygenated, preheated to 37 °C, filtered by a bubble trap and finally pumped by a peristaltic pump to the liver. 2 h later, the partial liver was excised for gene and protein analyses, and the others were fixed for immunofluorescence, immunohistochemistry, and H&E staining assays. Fractions of active caspase-3$^+$ and TUNEL$^+$ hepatocytes were counted to evaluate perfusion-induced apoptosis when the intraperitoneal injection of D-galactosamine/lipopolysaccharide and the DNase treatment were used as respective positive controls. For fluorescent particle diffusion tests, 0.2 mg/ml of FITC-labeled dextran (10 kDa; Sigma-Aldrich, MO) in phosphate-buffered saline (Hyclone, UT) was forced into the portal vein at 4 or 8 ml/min and recorded at 496/516 nm (excitation/emission) continuously by confocal laser-scanning microscopy (Zeiss LSM880, Germany). Dextran accumulation, defined by fluorescence intensity, was measured using imageJ software (National Institutes of Health, MD).

Microfluidic device fabrication

The microfluidic device was constructed using soft lithography as described previously,[7] serving as a hepatic sinusoid chip for *in vitro* tests in this work. Briefly, a silicon-wafer SU-8 template (Capital Bio Corporation, China) was used as a negative mold to generate a polydimethylsiloxane (PDMS; Dow Corning, MI) layer containing a channel with dimensions of 100 μm × 1 mm × 10 mm (height × width × length). The PDMS layer was bonded firmly to the glass coverslip after both PDMS and glass were treated using Plasma Sputtering Pump (Yilibotong, China) for 1 min. The integrated device was UV-sterilized for 30 min, and the channel was coated with 100 μg/ml of collagen I at 37 °C overnight before use. Cell suspension was then injected into the channel at a concentration of 1.0 × 10^7 cells/ml and dead cells were washed away 4 h later.

Statistical analysis

The *p* values were calculated using the two-tailed *t*-test for any two groups if passing the normality test (Shapiro-Will) or using the Mann-Whitney *U* test if not. For multiple group comparisons, we implemented the two-way ANOVA test followed by Holm-Sidak test, the one-way ANOVA test followed by Holm-Sidak test (if passing the normality test), or the Kruskal-Wallis one-way analysis of variance on ranks followed by Dunn's test (if not passing the normality test). Statistical significance was set at $p < 0.05$. n values in those figure captions denoted the number of independent repetitions. Specifically in animal tests, n indicated the number of mice included per condition.

Other relevant materials and methods are provided in the supplementary information and CTAT methods table.

Results

Hepatic flow alteration triggered hepatocyte proliferation *ex vivo*

Emerging evidence indicates the potential role of blood flow in liver regeneration after PHx. To evaluate if hepatocyte proliferation could be regulated by flow-induced mechanical alterations, mouse livers were perfused with Krebs–Henseleit buffer in the absence of growth factors at a flow rate of 4 or 8 ml/min for 2 h to mimic physiological and hepatectomized conditions,[6,18] respectively. H&E staining indicated that the anatomical structure was kept intact without significantly necrotic tissues (*upper panel* in Fig. 1A). Quantitative analysis of active caspase-3$^+$ cells% and TUNEL$^+$ cells% indicated that few apoptotic hepatocytes were induced by liver perfusion (Fig. 1A–C). Taking cyclin D1 as a typical marker to identify proliferative cells,[19,20] a higher flow rate of 8 ml/min led to more cyclin D1$^+$ cells which were colocalized with albumin-expressing hepatocytes (Fig. 1D). In addition, expressions of those genes associated with the cell cycle, such as *Ccna2*, *Ccnb1*, *Ccnd1*, *Ccne1*, *Cdk1* and *Mki67* (encoding cyclin A2, cyclin B1, cyclin D1, cyclin E1, cyclin-dependent kinase 1 [Cdk1] and Ki-67, respectively) were also higher at 8 ml/min than those at 4 ml/min (Fig. 1E). To quantify protein level changes, a capillary-based immunoassay was used to test the expression of cyclin D1 and its catalytic partner, Cdk4, both of which are known to form an essential heterodimeric complex that drives cell cycle entry and progression.[21] Protein expression of cyclin D1 and Cdk4 supported their relevant mRNA data, also

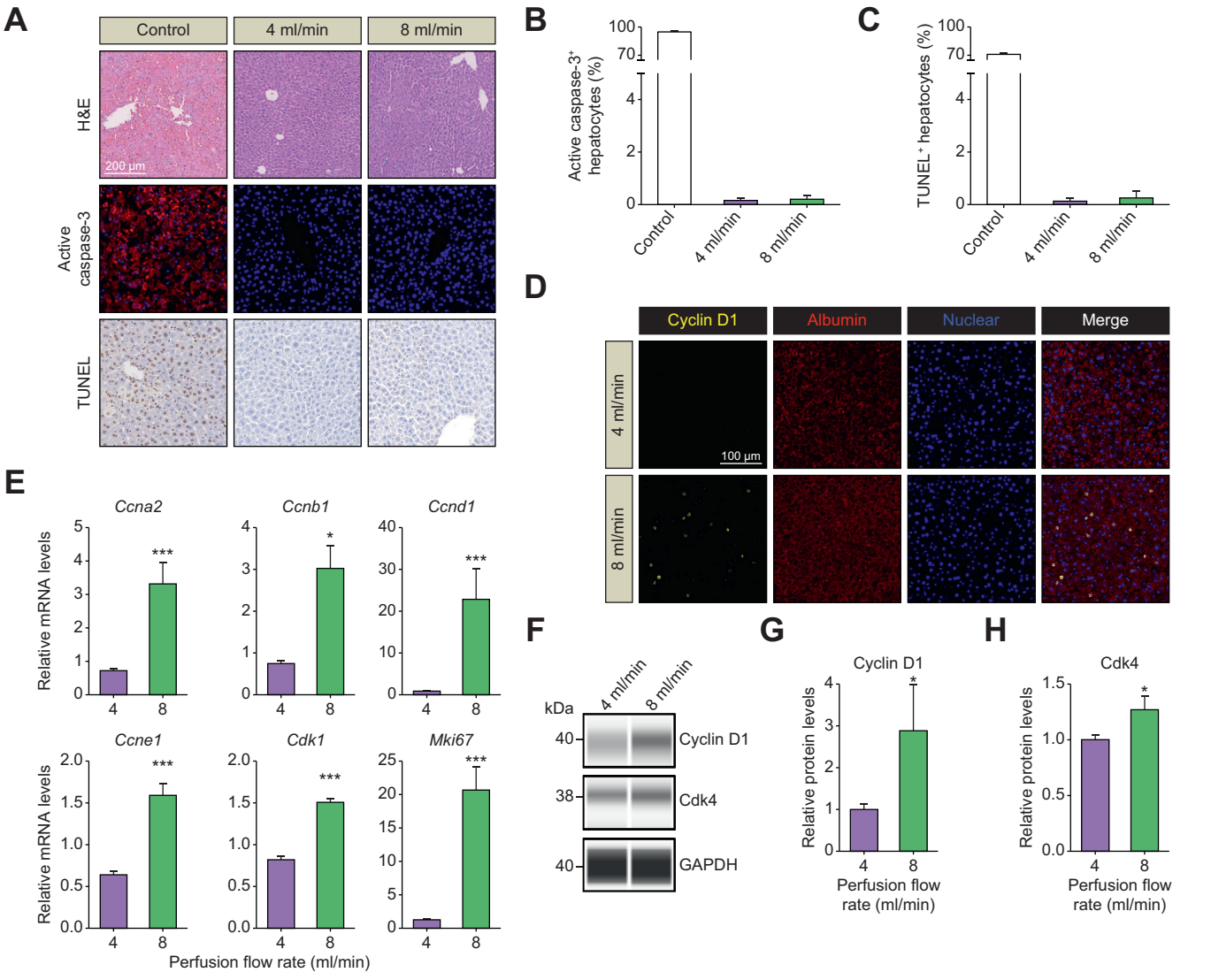

Fig. 1. ***Ex vivo*** **liver perfusion was correlated with hepatocyte proliferation.** (A–C) Representative images of H&E, active caspase-3, and TUNEL staining (A), and relevant quantitative analysis of active caspase-3$^+$ cells% (n = 3) (B), and TUNEL$^+$ cells% (n = 3) (C). D-galactosamine/lipopolysaccharide-damaged liver served as positive control for H&E and active caspase-3 tests. DNase-treated tissue served as a positive control for TUNEL staining. (D) Immunofluorescence co-staining of cyclin D1 and albumin (n = 3) in livers perfused *ex vivo* at a flow rate of 4 ml/min or 8 ml/min. (E) Expression of cell cycle relevant genes analyzed by RT-PCR at 8 ml/min compared with those at 4 ml/min (n = 6). (F–H) Protein level expression was determined by capillary-based immunoassay (F) with relevant quantitative analysis of cyclin D1 (n = 6) (G) and Cdk4 (n = 6) (H). Data were presented as mean ± SE. p <0.05*, 0.001***. Statistical analysis was performed by two-tailed t test for Ccne1 in E, and by Mann-Whitney U test for other markers in E, G, H.

being enhanced at 8 ml/min (Fig. 1F–H). Collectively, these results suggested that increased perfusion aroused hepatocytes in the quiescent G0 state to re-enter the cell cycle in the absence of the potential contributions of blood constituents.

Hepatocytes were exposed directly to interstitial flow in the space of Disse

Although extensive studies have attributed hepatocyte proliferation to those mitogenic factors released by non-parenchymal cells,[2] the liver sinusoids are highly fenestrated, which allows blood flow to drive interstitial flow in the space of Disse. Based on the previous observations that mechanical forces play a role in liver regeneration,[3] herein, we hypothesized that PHx-induced interstitial flow changes in the space of Disse might contribute to initiating liver regeneration, starting from hepatocyte proliferation via mechanosensitive pathways. To visualize the interstitial flow, blood vessels (*red*) in the freshly isolated mouse liver were stained with tomato lectin and hepatocytes (*cyan*) were depicted by their autofluorescence (Fig. 2A). The lobule structure was clearly presented where the enlarged area illustrated the well-distributed hepatic plates and sinusoids. Subsequently, 0.2 mg/ml FITC-labeled dextran (10 kDa) solution was introduced into the liver via the portal vein at 4 ml/min and monitored at different time points (Fig. 2B and Movie S1). The labeled dextran first appeared in the liver sinusoids and then diffused into the hepatocyte plate region about 2 min after perfusion. To exclude the deviation resulting from anatomical microstructures, the identical position was chosen for visualizing dextran diffusion at a high perfusion rate of 8 ml/min (Movie S1) after washing dextran away. Serial-shot images revealed that the diffusion process was accelerated as indicated by fast dextran appearance outside of sinusoids (~1 min after perfusion) and brightened in

the hepatocyte plate region at the same time point, demonstrating the high permeability of the sinusoidal lumen in contrast to the well-established barrier function of large vessels.[22] Indeed, the dextran tended to diffuse from microvessels (shown by dotted lines) towards hepatocytes (left panel in Fig. 2C). Together with the gradually reduced fluorescence intensity from inside to outside the liver sinusoid, as revealed by the heatmap using ImageJ software (right panel in Fig. 2C), this perfused fluid was inferred to be capable of physically contacting hepatocytes through the endothelium. In addition, quantitative analysis exhibited significantly higher and faster dextran accumulation outside of liver sinusoids after perfusion at 8 ml/min compared with 4 ml/min (Fig. 2D). The ratio of dextran accumulation from outside to inside the liver sinusoids decreased with time and finally reached a plateau (Fig. 2E). Here, the higher perfusion rate was associated with a more rapid descending phase, consistent with the high permeability interstitial flow at the high perfusion rate. By contrast, the steady state remained the same at both perfusion rates, indicating that the permeability coefficient determined by sinusoidal microstructure was not altered significantly during this perfusion process. Meanwhile, the diameter of liver sinusoids yielded no significant changes before and after 5 min of perfusion at both 4 and 8 ml/min (Fig. 2F and G), implying no differential expansion of the sinusoidal lumen at the two perfusion rates. Collectively, these results suggested that hepatocytes could be exposed to interstitial flow and the flow rate inside the space of Disse was increased with increasing perfusion rate. Hence, our cell proliferation data (Fig. 1) together with dextran perfusion observations (Fig. 2), indicate that hepatocyte proliferation could be initiated by perfusion-induced mechanical alterations, such as the enhanced interstitial flow in the liver.

Supplementary video related to this article can be found at https://doi.org/10.1016/j.jhepr.2023.100905

Shear stress initiated hepatocyte proliferation *in vitro*

Inspired by the above *ex vivo* liver perfusion readouts, we next tested whether flow-induced shear stress could favor hepatocytes to re-enter the cell cycle *in vitro*. Here hepatocytes were introduced into a hepatic sinusoid chip (Fig. 3A) and exposed to

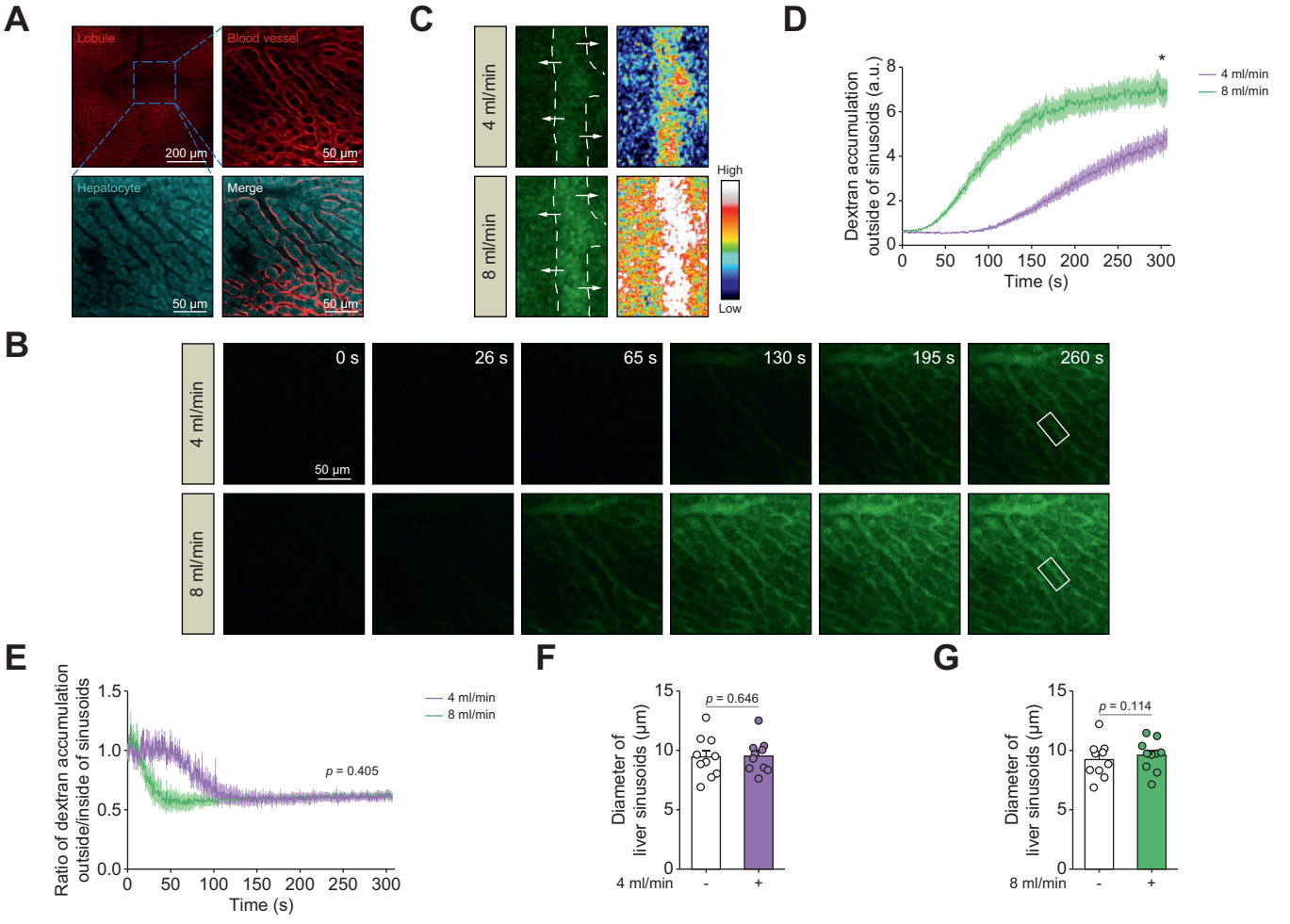

Fig. 2. Interstitial flow sensed by hepatocytes increased with perfusion rate. (A) Images of blood vessel staining with tomato lectin (red) and hepatocytes visualized by autofluorescence (cyan). (B) Time course of FITC-labeled dextran (10 kDa) diffusion was monitored at the identical position (rectangle in A) at various flow rates. (C) Enlarged images of the identical liver sinusoid from the rectangles denoted in B. Dotted lines and arrows in left panel indicated the microvessel profiles and diffusion directions, respectively. Right panel presented the heatmap of fluorescence intensity measured. (D, E) Quantitative analysis of dextran accumulation outside (n = 5) (D) or outside/inside ratio of the liver sinusoids (n = 5) (E). (F, G) Diameter of liver sinusoids before and after liver perfusion at 4 ml/min (n = 10) (F) or 8 ml/min (n = 10) (G). Data were presented as mean ± SE. p <0.05*. Statistical analysis was performed by two-tailed t test in D-G.

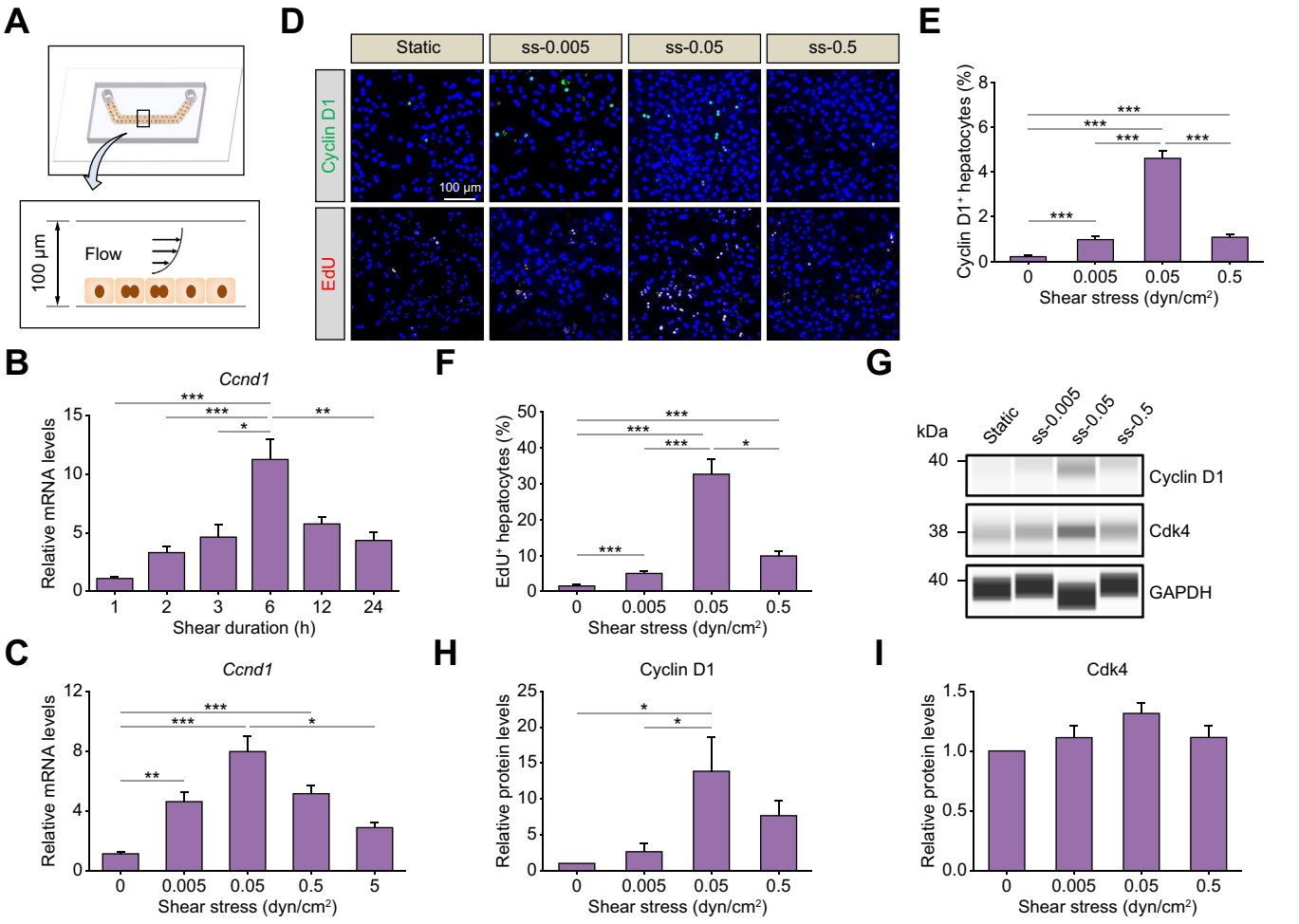

Fig. 3. Shear stress alone initiated hepatocyte proliferation *in vitro*. (A) Schematic diagram of an in-house developed hepatic sinusoid chip. (B, C) Expression of cyclin D1 gene in mouse primary hepatocytes, after exposure to a given shear stress at 0.05 dyn/cm^2 with varied durations (n = 3∼6) (B) or to varied shear stresses at given duration of 6 h (n = 3∼10) (C). (D–F) Typical images of proliferative hepatocytes (D) and relevant quantitative analysis of cyclin D1$^+$% (n = 3) (E) and EdU$^+$% cells (n = 3) (F) at varied shear stresses for 6 h. (G–I) Protein level expression was determined by capillary-based immunoassays at varied shear stresses for 6 h (G) with relevant quantitative analysis for cyclin D1 (n = 3) (H) and Cdk4 (n = 5) (I). Data were presented as mean ± SE. p <0.05*, 0.01**, 0.001***. Statistical analysis was performed by one-way ANOVA followed by Holm-Sidak test in H, I, and by Kruskal-Wallis one-way analysis of variance on ranks followed by Dunn's test in B, C, E, F. Cdk4, cyclin-dependent kinase 4; ss-0.005/0.05/0.5, shear stress-0.005/0.05/0.5 dyn/cm^2.

flow shear first at a given shear stress of 0.05 dyn/cm^2 with systematically varied durations (1, 2, 3, 6, 12, and 24 h) (Fig. 3B). Cyclin D1 gene expression increased with time to peak at 6 h and then declined, demonstrating the vital role of shear duration in controlling the cell cycle. To evaluate how shear amplitude affected cell proliferation, hepatocytes were exposed to varied shear stresses (0, 0.005, 0.05, 0.5, and 5 dyn/cm^2) for a given duration of 6 h (Fig. 3C). Again, cyclin D1 gene expression increased with shear stress to peak at 0.05 dyn/cm^2 and then decreased, implying the key role of shear amplitude in modulating the cell cycle. To further validate this finding, hepatocyte proliferation was characterized by cyclin D1 and EdU staining (an S phase marker) after exposure to various shear stresses for 6 h (Fig. 3D). Quantitative analysis demonstrated that maximum positive cell ratio was observed at 0.05 dyn/cm^2 (Fig. 3E and F). Consistently, protein levels of cyclin D1 and Cdk4 exhibited similar expression profiles (Fig. 3G–I). Thus, these results suggested that flow-induced shear stress was able to initiate hepatocyte proliferation *in vitro*, which was regulated cooperatively by shear duration and shear amplitude with an optimized parameter set at 0.05 dyn/cm^2 for 6 h.

Physiologically, after PHx, remaining hepatocytes are required not only to maintain sufficient proliferation but also to meet hepatic metabolic demands. In this work, a hepatocyte-specific phenotype was further evaluated after *in vitro* shear stress exposure. Typical functional genes including *Alb*, *Cyp3a11*, *Cyp1a2*, *Por*, *Glul*, and *Hnf4a* were increased, or maintained at least, when applying shear stress (Fig. S1A). Albumin production in the collected supernatant was also elevated by shear stress exposure (Fig. S1B). In concordance with this data on gene expression, the capabilities for cellular detoxication and metabolism were validated by immunostaining CYP1A2 and CYP3A11 (Fig. S1C); the metabolic activity of CYP3A11 was induced after the exposure, especially by dexamethasone induction (Fig. S1D). In addition, glycogen accumulation and bile canaliculi network formation were observed in both 0.05 dyn/cm^2 for 6 h (ss-0.05) and static groups (Fig. S1E and F). Hepatocytes were also exposed at various concentrations of alcohol to test their resistance

capability to liver injury. Results indicated that shear stress significantly improved cell survival rate under each alcohol concentration compared with static control, implying a protective role of flow shear in alcohol-induced apoptosis (Fig. S1G). In summary, shear stress exposure was able to maintain hepatic functions when initiating hepatocyte proliferation.

To find out how hepatocytes responded to shear stress and initiated proliferation, RNA-seq was performed for hepatocytes in the ss-0.05 and static control groups. KEGG analysis showed that 40% of items were involved in cell growth and death among the top 10 enriched cellular processes for differentially expressed genes between the two groups (Fig. 4A). Gene ontology classification indicated that there were more upregulated genes than downregulated ones in most biological processes (Fig. 4B). Specifically, cell-proliferation-relevant genes were differentially expressed (Fig. 4C). Further analysis implied that typical liver progenitor/cholangiocyte markers of *Krt19*, *Epcam*, *Sox4* and *Cd44* were upregulated in the ss-0.05 group (Fig. 4D), accompanied by increased expression of the typical proliferation markers *Ccnd1*, *Top2a* and *Aurkb* (Fig. 4E). This was also confirmed by qPCR analysis of enhanced cell cycle-dominant genes, namely *Ccna2*, *Ccne1*, *Cdk1* and *Mki67* (Fig. 4F). Collectively, these data suggested that shear stress favored hepatocytes to acquire a progenitor phenotype and express cell cycle-regulating markers to initiate their proliferation.

YAP activation was required for shear-initiated hepatocyte proliferation

To explore the underlying mechanism of shear-initiated proliferation, the upregulated genes involved in cell proliferation shown in Fig. 4C were further analyzed by KEGG. Top 10 lists showed that Hippo was the second most enriched signaling pathway (Fig. 5A). Hippo/YAP signature genes were differentially regulated between ss-0.05 and static groups (Fig. 5B), as expected. Meanwhile, significantly higher expression of classic YAP target genes was observed in the ss-0.05 group (Fig. 5C). Expression of YAP and its target genes, determined by qPCR, supported RNA-seq data (Fig. 5D). Consistently, protein level expression of p-YAP/YAP was downregulated, confirming YAP activation under shear stress (Fig. 5E).

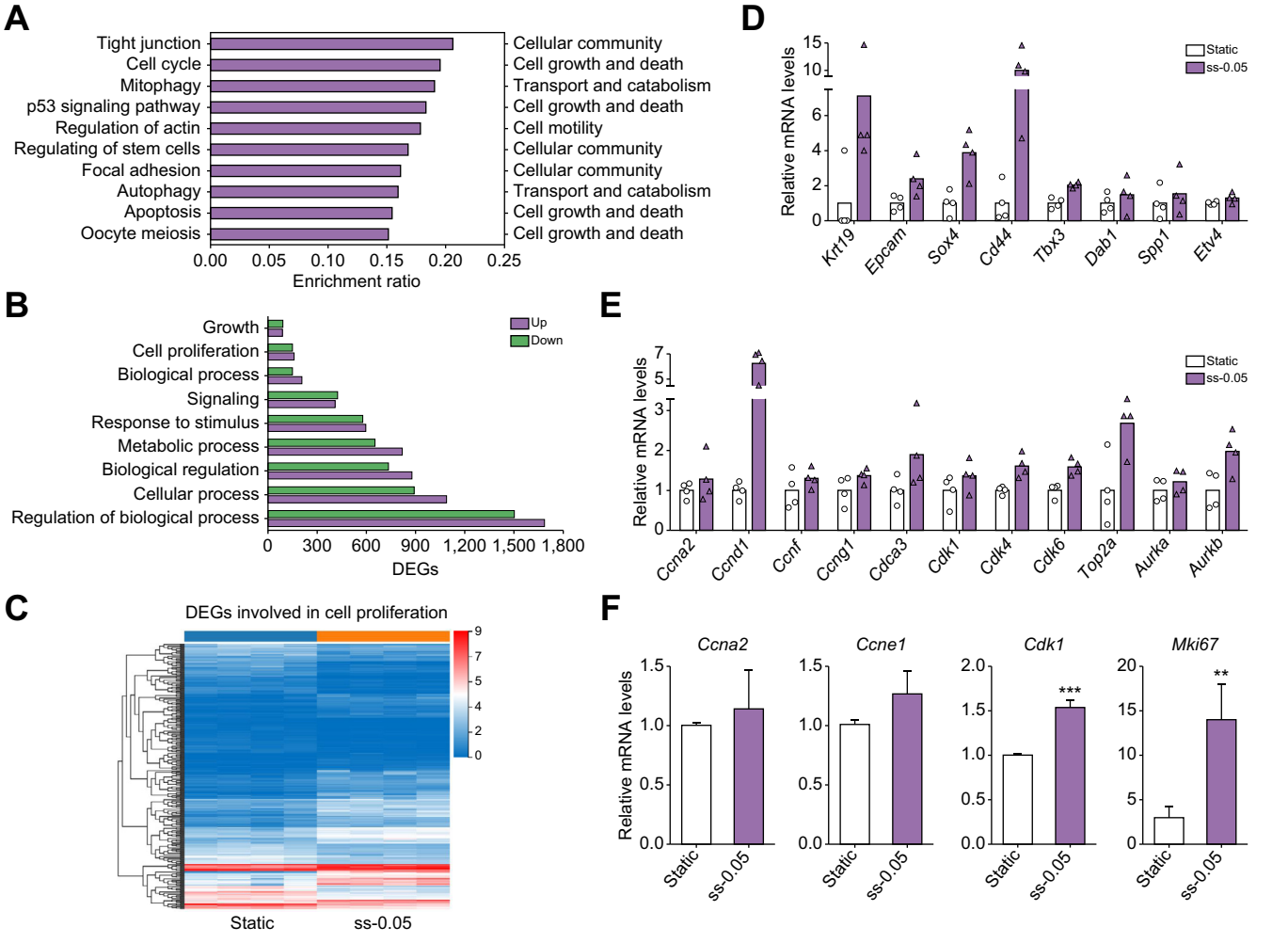

Fig. 4. Hepatocytes tended to present a progenitor phenotype in response to shear stress. (A) KEGG pathway enrichment analysis for the DEGs between ss-0.05 group and static control. Left and right y-axis denoted the top 10 enriched items involved in cellular processes and their corresponding classifications in the KEGG database, respectively. (B) DEG numbers in different biological processes based on GO classification. (C) Heatmap visualization of DEGs related to cell proliferation shown in B. (D, E) Gene expression profiles of typical liver progenitor/cholangiocyte markers (n = 4) (D) and proliferation markers (n = 4) (E) measured by RNA-seq. (F) Expression of cell cycle-relevant genes analyzed by RT-PCR (n = 3∼4). Data were presented as mean ± SE. p <0.05*, 0.01**, 0.001***. Statistical analysis was performed by two-tailed t test for Ccne1 and by Mann-Whitney U test for other markers in F. ss-0.05, shear stress-0.05 dyn/cm^2.

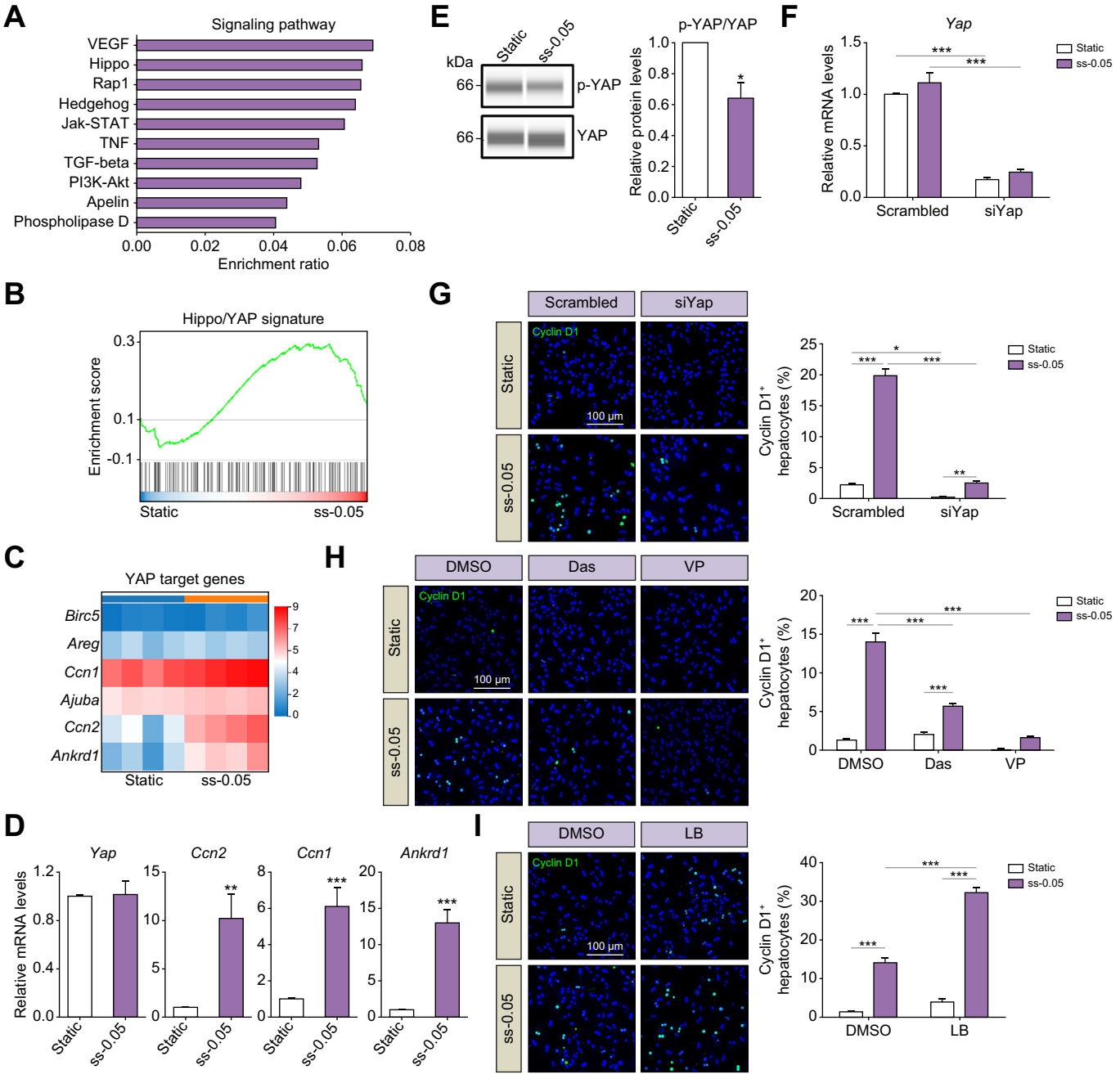

Fig. 5. YAP was required for shear-initiated hepatocyte proliferation. (A) Top 10 signaling pathways enriched by KEGG based on upregulated DEGs in Fig. 3C. (B) Gene set-enrichment analysis of DEGs related to Hippo/YAP pathways. (C) Heatmap summarizing the expression of classical YAP target genes. (D) Expression of YAP and its target genes evaluated by RT-PCR (n = 3~4). (E) Expression of phosphorylated and total YAP determined by capillary-based immunoassays (left). Densitometric analysis was performed by p-YAP/YAP (right) (n = 3). (F) Gene expression of YAP after siRNA transfection (n = 4). (G–I) Representative images of cyclin D1 (left) and relevant quantitative analysis of positive cell ratio (right) when hepatocytes were treated with YAP siRNA (n = 3) (G), Das (n = 5), VP (n = 5) (H), or LB (n = 4) (I) between ss-0.05 group and static control. Data were presented as mean ± SE. p <0.05*, 0.01**, 0.001***. Statistical analysis was performed by Mann-Whitney U test for Ccn2 in D, by two-tailed t test for other markers in D, E, and by two-way ANOVA followed by Holm-Sidak test in F–I. Das, dasatinib; LB, leptomycin B; siYap, siRNA targeting YAP; ss-0.05, shear stress-0.05 dyn/cm^2; VP, verteporfin.

To elucidate whether YAP was required for shear-initiated hepatocyte proliferation, the hepatocytes were transfected with siRNA targeting YAP (siYap). Gene expression of both YAP and its target genes *Ccn2*, *Ccn1* and *Ankrd1* were significantly reduced by siRNA transfection (Fig. 5F and Fig. S2A). Immunostaining (left) and quantitative analysis (right) revealed that the cyclin D1$^+$ ratio declined after YAP knockdown (Fig. 5G). Moreover, expression of cell cycle-related genes (*Ccna2*, *Ccnd1*, *Cdk1* and *Mki67*) was also downregulated in the siYap group (Fig. S2B). Consistently, when hepatocytes were treated with 20 μM dasatinib or 20 μM verteporfin for 12 h to inhibit YAP activation,[23,24] both the expression of YAP target genes and cell cycle-related genes, as well as the cyclin D1$^+$ ratio, were reduced (Fig. S3 and Fig. 5H). By contrast, the addition of leptomycin B, a

potent inhibitor of the nuclear export of proteins,[25] significantly elevated cyclin D1$^+$ ratio (Fig. 5I). These results suggested that YAP activation was required for shear-initiated hepatocyte proliferation *in vitro*.

β1 integrin sensed shear stress and maintained YAP-dependent hepatocyte proliferation

We further explored how hepatocytes sensed shear stress on the cell membrane and mediated intracellular mechanotransduction, since YAP can only impel cell cycle progression by binding DNA in the nucleus. We first tested the integrin sensitivity of hepatocytes in response to shear stress and data indicated that gene and protein expressions of β1 integrin were all upregulated (Fig. 6A–C). Subsequently, transfecting the cells with siRNA targeting β1 integrin (siltgb1) significantly reduced β1 integrin gene expression, cyclin D1$^+$ ratio, and expression of *Ccna2*, *Ccnd1*, and *Mki67* (Fig. 6D and E, and Fig. S4A). On the contrary, treating cells with pyrintegrin, an agonist to promote β1 integrin expression, increased cyclin D1$^+$ ratio (Fig. S4B). Furthermore, YAP target genes were downregulated by integrin knockdown (Fig. 6F). To determine the interplay between YAP and integrin partners, we treated hepatocytes with dasatinib, which did not affect β1 integrin expression (Fig. S4C), implying that β1 integrin served as an upstream regulator of YAP signaling. These results indicated that YAP activation and the initiation of hepatocyte proliferation in response to shear stress were associated with β1 integrin signaling.

FAK was involved in the mechanotransduction of YAP via the Hippo pathway

Mechanical signals sensed by integrins are transmitted towards the intracellular region via its major downstream effectors, FAK and integrin-linked kinase,[26] which may serve as the connecting player(s) between β1 integrin and YAP. Herein, protein expression of p-FAK/FAK was notably induced by shear stress (Fig. 7A). In addition, FAK knockdown with siRNA transfection (siFak) reduced *Fak* gene expression, cyclin D1$^+$ ratio, and expression of *Ccna2, Ccnd1,* and *Mki67* (Fig. 7B and C, and Fig. S5). YAP target genes (*Ccn2*, *Ccn1* and *Ankrd1*) were also downregulated by FAK siRNA transfection (Fig. 7D). To evaluate whether FAK signaling regulated YAP-dependent hepatocyte proliferation via the classical Hippo pathway, the core component of Hippo, LATS, was tested along this signaling cascade.[27] Results indicated that p-LATS/LATS expression declined in response to shear stress and

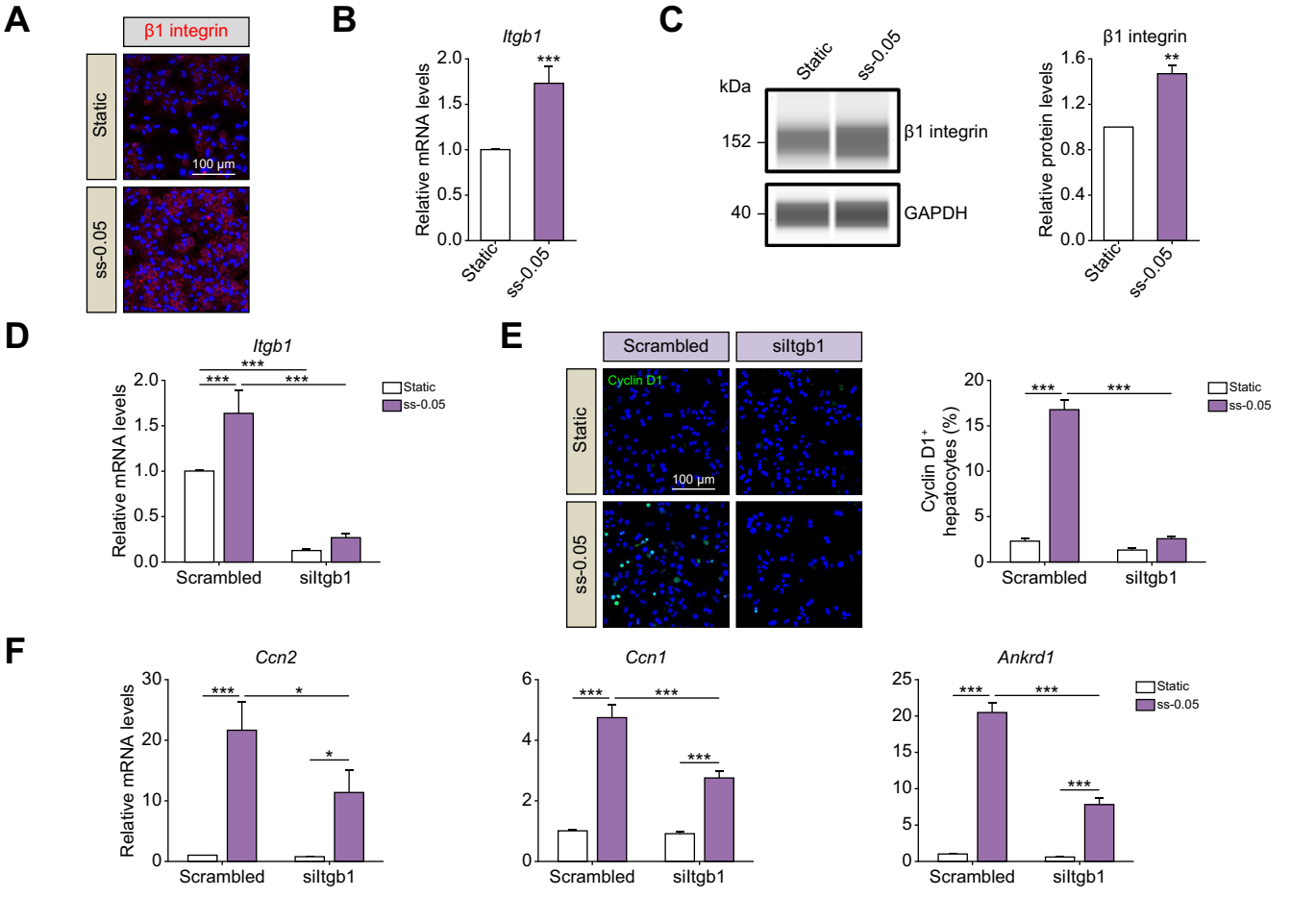

Fig. 6. β1 integrin facilitated YAP-dependent hepatocyte proliferation in response to shear stress. (A-C) Representative images of β1 integrin (A) and its gene (n = 7) (B) or protein expression (n = 3) (C) after exposure to shear stress. (D) Gene expression of β1 integrin after siRNA transfection (n = 5). (E) Representative images of cyclin D1 and relevant quantitative analysis of positive cell ratio when hepatocytes were transfected with β1 integrin siRNA (n = 4). (F) Expressions of YAP target genes after siRNA transfection, determined by RT-PCR (n = 4∼5). Data were presented as mean ± SE. p <0.05*, 0.01**, 0.001***. Statistical analysis was performed by Mann-Whitney *U* test in B, by two-tailed *t* test in C, and by two-way ANOVA followed by Holm-Sidak test in D-F. siltgb1, siRNA targeting β1 integrin; ss-0.05, shear stress-0.05 dyn/cm^2.

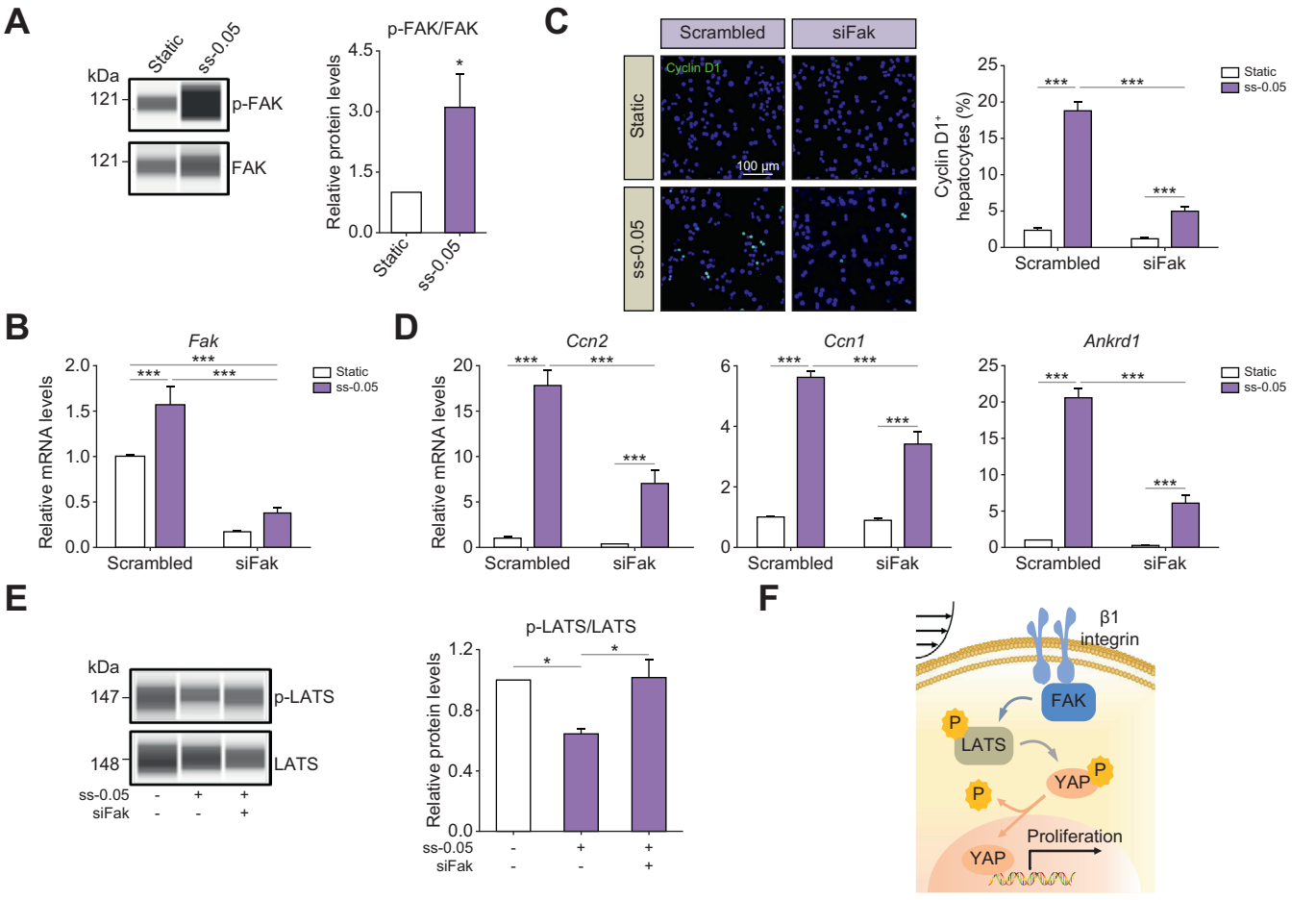

Fig. 7. FAK signaling promoted the mechanotransduction from β1 integrin to YAP through the Hippo pathway. (A) Protein expression of phosphorylated and total FAK. Densitometric analysis was performed by p-FAK/FAK (n = 5). (B) Gene expression of FAK after siRNA transfection (n = 6). (C) Representative images of cyclin D1 and relevant quantitative analysis of positive cell ratio when hepatocytes were transfected with FAK siRNA (n = 3). (D) Expression of YAP target genes after siRNA transfection, determined by RT-PCR (n = 3). (E) Protein expression of phosphorylated and total LATS in the absence or presence of FAK siRNA treatment (n = 5). Densitometric analysis was performed by p-LATS/LATS. (F) Schematic showing the regulatory effects of shear stress on hepatocyte proliferation. Data were presented as mean ± SE. p <0.05*, 0.01**, 0.001***. Statistical analysis was performed by two-tailed t test in A, by two-way ANOVA followed by Holm-Sidak test in B-D, and by one-way ANOVA followed by Holm-Sidak test in E. siFak, siRNA targeting FAK; ss-0.05, shear stress-0.05 dyn/cm^2.

was rescued by FAK siRNA transfection (Fig. 7E), indicating its role as a negative regulator of shear-initiated hepatocyte proliferation. These results indicated that FAK was involved in the cytoplasmic transmission of signals from β1 integrin to YAP through the Hippo signaling pathway (Fig. 7F).

Discussion

Hepatocyte proliferation is vital *in vivo* for liver regeneration after PHx and critical *in vitro* for liver repair after injury. A single hepatocyte can expand through a maximum number of 34 divisions after PHx but loses its proliferative ability in *in vitro* culture, resulting in a shortage of hepatocytes for transplantation, bioartificial liver construction, and clinical research.[28] Inspired by the instant dramatic hemodynamic alterations during PHx-induced liver regeneration, we tested if interstitial flow-driven shear stress in the space of Disse could initiate hepatocyte proliferation. Interestingly, primary mouse hepatocytes were able to re-enter the cell cycle, which was induced not only by *ex vivo* liver perfusion but also the application of *in vitro* shear stress in the absence of growth factors. Expression of genes related to liver progenitors/cholangiocytes were upregulated accordingly, consistent with previous findings that regenerative hepatocytes after PHx were reprogrammed into an early postnatal-like state before proceeding toward the proliferative trajectory.[29] Thus, this work provided new insights into initiating primary hepatocyte proliferation *in vitro* and could presumably contribute to cell expansion in cooperation with other culture methods like liver organoid construction.

Emerging evidence suggests that mechanical forces play an important role in the regenerative process.[2] For example, LSECs that line hepatic sinusoids first sense blood flow changes, which are followed by increased sinusoidal diameter, enlarged cellular fenestrae and widened intercellular junctions after PHx.[30] Uniaxial stretched LSECs are able to secrete more HGF to promote hepatocyte proliferation.[6] In response to shear stress, LSECs release nitric oxide to reinforce hepatocytes' sensitivity to HGF.[31] Hepatic stellate cells (HSCs), which reside within the space of Disse, are associated with synaptic-type connections to both hepatocytes and LSECs.[32] They are also exposed to interstitial flow, like hepatocytes, and subjected to mechanical tension produced by the extracellular matrix.[33] Reduction in

interstitial flow in the liver tissue of aged mice yields less HGF, whereas both shear stress and mechanical stretch *in vitro* promote HGF release from HSCs.[34] Undoubtedly, these paracrine biochemical factors secreted from non-parenchymal cells are able to significantly promote liver regeneration. Taking the rapid regenerative response after PHx within seconds into consideration, several fast-phase changes on hepatocytes themselves may also participate in initiating liver regeneration and lead hepatocytes to enter the cell cycle, like membrane potential alterations of hepatocytes (within minutes).[35] Meanwhile, since hepatocytes are known as mechanosensitive cells, another possibility is that hepatocyte proliferation is triggered by mechanical loading on hepatocytes directly. Combined with our direct observations of interstitial flow in the space of Disse, these results proposed that shear stress exposure was able to stimulate hepatocytes to enter the cell cycle from a quiescent state and thus initiate the liver regeneration process together with various biochemical factors.

Cell cycle entry is driven by the formation of cyclin D and cyclin-dependent kinase complexes.[21] In hepatocytes, cyclin D1 is markedly synthesized and accumulated in G1 phase, the first phase of the cell cycle, and reduced to low levels before entering S phase.[36] It can activate Cdk4 to promote the expression and activation of other cyclin/cyclin-dependent kinase complexes that contribute to cell cycle progression through subsequent phases,[19] thus serving as a promising candidate for the initiation of cell proliferation. In our *in vitro* model, cyclin D1 was upregulated by shear stress exposure and presented time-dependent expression where it peaked at 6 h and declined thereafter. Of note, two-thirds PHx *in vivo* led to a peak in cyclin D1 expression at 24-48 h post hepatectomy.[37] There are a couple of potential explanations for this time-window shifting of cyclin D1 expression. First, PHx not only initiates the liver regeneration process but also activates those signaling pathways related to its termination in case of excessive growth, including the pathway mediated by TGF-β1 (produced by non-parenchymal cells) or extracellular matrix (synthesized by HSCs).[38] In contrast, the absence of those paracrine mitogenic inhibitors like TGF-β1 in our *in vitro* isolated hepatocyte model may result in an earlier peak time point. Second, this earlier time point of 6 h is also likely to be the specific peak in response to shear stress *in vitro* rather than the mechano-biochemical coupling stimuli *in vivo*. It is assumed that supplementation of biochemical factors originating from PHx would lead to consistent responses in hepatocytes *in vitro* and *in vivo*, though this warrants further verification.

Intrahepatic shear stress is hard to measure experimentally due to the tiny radius of sinusoids and the varying viscosity within the liver, especially for the interstitial flow within the narrow space of Disse.[31,39] In this *in vitro* test, hepatocytes were exposed to varied shear stress from 0.005 to 5 dyn/cm^2, based on summarized parameters from the literature.[40] Interestingly, applying shear stress *in vitro* yielded a biphasic effect on hepatocyte proliferation, that is, hepatocyte proliferation was favored at the threshold stress of 0.05 dyn/cm^2 while other lower or higher values all presented confined benefits, consistent with previous observations that an appropriate perfusion rate promoted cell proliferation to achieve the best output in the decellularized liver scaffold.[41] This finding may also account for the insufficient cell division following relatively low shear stress after 30% PHx and also for small-for-size syndrome following extremely high shear stress after extended hepatectomy or liver transplantation using small-sized grafts.[30] In fact, hepatocyte proliferation is not homogeneous throughout the liver after PHx. Hepatocytes usually start to proliferate in the periportal region,[42] while liver homeostasis is mainly maintained by midlobular hepatocytes.[43] This inhomogeneous proliferation seems positively correlated to sinusoidal blood flow distribution, since flow velocity increases gradually from the periportal to pericentral region, as measured by leukocyte movement in different sinusoidal zones with intravital microscopy.[44] Interestingly, LSEC permeability is also increased from the periportal to pericentral region, as determined by increased porosity of fenestrae.[45] Considering that the shear stress is proportional to the flow velocity of interstitial flow, it seems meaningful that the position of optimal shear stress for hepatocyte proliferation is located at midlobular region during liver homeostasis but shifted to the periportal region during liver regeneration, after blood flow is increased by PHx.

Hepatocyte proliferation could be accomplished *in vitro* to a certain extent, although little is known about the underlying molecular mechanism. For example, an *in vitro* 3D spheroid model of primary human hepatocytes recapitulates the *in vivo* regenerative phenotype upon PHx.[46] Based on analyzing global promoter motif activities, Wnt/β-catenin activation and p53 signaling inhibition have been identified as critical factors for primary human hepatocyte proliferation. In response to mechanical modulation, 3D organoid culture triggers two waves of proliferation induced by matrix stiffness and cell-cell interactions via the MER1/2-ERK1/2 signaling pathway.[20] To the best of our knowledge, primary hepatocyte proliferation initiated by shear stress *in vitro* has not been studied yet, although immediate early gene expression is increased in hepatic cell lines under laminar or interstitial flow.[39,47] Furthermore, our results indicated that shear stress stimulated hepatocytes to re-enter the cell cycle in a YAP-dependent manner, regulated by β1 integrin through the Hippo signaling pathway.

Intracellular mechanotransductive pathways are crucial to understand the underlying mechanisms in shear-initiated hepatocyte proliferation. As to the sensation of extracellular mechanical signals, our results indicated that β1 integrin knockdown or activation significantly weakened or strengthened shear-initiated hepatocyte proliferation, respectively, indicating the key role of β1 integrin as a shear sensor on the cell membrane. These observations were also consistent with the findings that shear-activated integrin-FAK signaling regulates HCC migration in a time-dependent manner.[48] Subsequent signal transmission from the cell membrane to the intracellular region is known to be mainly mediated by focal adhesions or cytoskeletons once perceived by integrins. Consistently, our data indicated that FAK knockdown broke up integrin-YAP signaling transduction and further reduced proliferative responses related to YAP shuttle. As to the intranuclear responses, activated YAP is able to translocate into the nucleus and initiate the transcription of various effector molecules. For example, aerobic glycolysis-regulated HCC migration relies on stiff matrix-induced YAP nuclear translocation.[49] Accordingly, our work indicated that YAP-dependent hepatocyte proliferation was impaired by either YAP knockdown or inactivation but enhanced by YAP activation, identifying YAP as a key player in shear-initiated hepatocyte proliferation. In fact, while the β1 integrin-FAK-YAP pathway has been extensively explored in HCC, how it works in primary hepatocytes is poorly understood. Moreover, β1 integrin and YAP have previously been shown to be essential for liver

regeneration,[14,17] but their roles in regulating shear-initiated hepatocyte proliferation were unknown. Intriguingly, we show that β1 integrin could activate YAP-dependent hepatocyte proliferation under shear stress, providing potential targets for establishing primary hepatocyte expansion *in vitro*.

In this work, mouse livers were perfused *ex vivo* and hepatocyte proliferation was found to be initiated at a high flow rate. Inspired by this observation, primary hepatocytes were exposed to shear stress *in vitro* in a hepatic sinusoid chip. Results indicated that direct exertion of shear stress indeed initiated proliferation, in a shear duration- and amplitude-dependent manner. The underlying mechanotransductive pathway involved the β1 integrin-FAK-Hippo-YAP signaling axis, driving hepatocytes to re-enter the cell cycle. These findings provide new insights into the mechanisms triggering liver regeneration *in vivo* and potentiating hepatocyte expansion *in vitro*.

Abbreviations

Cdk1/4, cyclin-dependent kinase 1/4; FAK, focal adhesion kinase; HCC, hepatocellular carcinoma; HGF, hepatic growth factor; HSCs, hepatic stellate cells; LSECs, liver sinusoidal endothelial cells; PDMS, polydimethylsiloxane; PHx, partial hepatectomy; TGF-β1, transforming growth factor β1; YAP, yes-associated protein.

Financial support

This work was supported by the National Natural Science Foundation of China Grants 32130061, 32271366 and 32101056, National Key R&D Program of China Grant 2021YFA0719300, China Manned Space Flight Technology Project Chinese Space Station Experiment Project YYW-T0901EXP0701 and the Scientific Instrument Developing Project and the Key Research Program of Chinese Academy of Sciences Grants GJJSTU20220002 and ZDBS-ZRKJZ-TLC002.

Conflict of interest

The authors declare no competing interests.

Please refer to the accompanying ICMJE disclosure forms for further details.

Authors' contributions

W Li, N Li, and M Long conceptualized and designed the study; W Li, ZL Zhang, Y Wu, J Zhou, XY Shu, and XY Zhang performed experiments; W Li, WH Hu, ZL Zhang and H Wu analyzed data; W Li, N Li, Y Du, DY Lü, SQ Lü, and M Long wrote the article.

Data availability statement

The data that support the findings of this study are available from the corresponding author upon reasonable request.

Supplementary data

Supplementary data to this article can be found online at https://doi.org/10.1016/j.jhepr.2023.100905.

References

Author names in bold designate shared co-first authorship

[1] Higgins GM, Anderson RM. Experimental pathology of the liver. I. Restoration of the liver of the white rat following partial surgical removal. Arch Pathol 1931;12(2):186–202.
[2] Michalopoulos GK, Bhushan B. Liver regeneration: biological and pathological mechanisms and implications. Nat Rev Gastroenterol Hepatol 2021;18(1):40–55.
[3] **Ishikawa J**, **Takeo M**, Iwadate A, Koya J, Kihira M, Oshima M, et al. Mechanical homeostasis of liver sinusoid is involved in the initiation and termination of liver regeneration. Commun Biol 2021;4(1):409.
[4] Iimuro Y, Kondo Y, Suzumura K, Uyama N, Asano Y, Hirano T, Yamanaka J, Iijima H, Nishiguchi S, Fujimoto J. Regional hepatic regeneration after liver resection correlates well with preceding changes in the regional portal circulation in humans. Dig Dis Sci 2013;58(10):3001–3009.
[5] **Christ B**, Collatz M, **Dahmen U**, **Herrmann KH**, Höpfl S, **König M**, **Lambers L**, **Marz M**, Meyer D, **Radde N**, **Reichenbach JR**, **Ricken T**, **Tautenhahn HM**. Hepatectomy-induced alterations in hepatic perfusion and function - toward multi-scale computational modeling for a better prediction of post-hepatectomy liver function. Front Physiol 2021;12:733868.
[6] **Lorenz L**, **Axnick J**, Buschmann T, Henning C, Urner S, Fang S, Nurmi H, Eichhorst N, Holtmeier R, Bodis K, Hwang JH, Mussig K, Eberhard D, Stypmann J, Kuss O, Roden M, Alitalo K, Haussinger D, Lammert E. Mechanosensing by beta1 integrin induces angiocrine signals for liver growth and survival. Nature 2018;562(7725):128–132.
[7] Li W, Li P, Li N, Du Y, Lü S, Elad D, Long M. Matrix stiffness and shear stresses modulate hepatocyte functions in a fibrotic liver sinusoidal model. Am J Physiol Gastrointest Liver Physiol 2021;320(3):G272–G282.
[8] Du Y, Li N, Yang H, Luo C, Gong Y, Tong C, Gao Y, Lu S, Long M. Mimicking liver sinusoidal structures and functions using a 3D-configured microfluidic chip. Lab Chip 2017;17(5):782–794.
[9] Yu F, Deng R, Hao Tong W, Huan L, Chan Way N, IslamBadhan A, Iliescu C, Yu H. A perfusion incubator liver chip for 3D cell culture with application on chronic hepatotoxicity testing. Sci Rep 2017;7(1):14528.
[10] Aragona M, Panciera T, Manfrin A, Giulitti S, Michielin F, Elvassore N, Dupont S, Piccolo S. A mechanical checkpoint controls multicellular growth through YAP/TAZ regulation by actin-processing factors. Cell 2013;154(5):1047–1059.
[11] **Song Z**, **Gupta K**, Ng IC, Xing J, Yang YA, Yu H. Mechanosensing in liver regeneration, Semin. Cell Dev. Biol 2017;71:153–167.
[12] **Schrader J**, **Gordon-Walker TT**, Aucott RL, van Deemter M, Quaas A, Walsh S, Benten D, Forbes SJ, Wells RG, Iredale JP. Matrix stiffness modulates proliferation, chemotherapeutic response, and dormancy in hepatocellular carcinoma cells. Hepatology 2011;53(4):1192–1205.
[13] **Desai SS**, **Tung JC**, Zhou VX, Grenert JP, Malato Y, Rezvani M, Espanol-Suner R, Willenbring H, Weaver VM, Chang TT. Physiological ranges of matrix rigidity modulate primary mouse hepatocyte function in part through hepatocyte nuclear factor 4 alpha. Hepatology 2016;64(1):261–275.
[14] Bhushan B, Molina L, Koral K, Stoops JW, Mars WM, Banerjee S, Orr A, Paranjpe S, Monga SP, Locker J, Michalopoulos GK. Yes-associated protein is crucial for constitutive androstane receptor-driven hepatocyte proliferation but not for induction of drug metabolism genes in mice. Hepatology 2021;73(5):2005–2022.
[15] Watkins RD, Buckarma EH, Tomlinson JL, McCabe CE, Yonkus JA, Werneburg NW, Bayer RL, Starlinger PP, Robertson KD, Wang C, Gores GJ, Smoot RL. SHP2 inhibition enhances yes-associated protein-mediated liver regeneration in murine partial hepatectomy models. JCI Insight 2022;7(15):e159930.
[16] Pocaterra A, Santinon G, Romani P, Brian I, Dimitracopoulos A, Ghisleni A, Carnicer-Lombarte A, Forcato M, Braghetta P, Montagner M, Galuppini F, Aragona M, Pennelli G, Bicciato S, Gauthier N, Franze K, Dupont S. F-actin dynamics regulates mammalian organ growth and cell fate maintenance. J Hepatol 2019;71(1):130–142.
[17] Speicher T, Siegenthaler B, Bogorad RL, Ruppert R, Petzold T, Padrissa-Altes S, Bachofner M, Anderson DG, Koteliansky V, Fässler R, Werner S. Knockdown and knockout of β1-integrin in hepatocytes impairs liver regeneration through inhibition of growth factor signalling. Nat Commun 2014;5:3862.
[18] Diaz-Juarez JA, Hernandez-Munoz R. Rat liver enzyme release depends on blood flow-bearing physical forces acting in endothelium glycocalyx rather than on liver damage. Oxid Med Cell Longevity 2017;2017:1360565.
[19] Wu H, Reizel T, Wang YJ, Lapiro JL, Kren BT, Schug J, Rao S, Morgan A, Herman A, Shekels LL, Rassette MS, Lane AN, Cassel T, Fan TWM, Manivel JC, Gunewardena S, Apte U, Sicinski P, Kaestner KH, Albrecht JH. A negative reciprocal regulatory axis between cyclin D1 and HNF4α modulates cell cycle progression and metabolism in the liver. Proc Natl Acad Sci U S A 2020;117(29):17177–17186.
[20] Rose S, Ezan F, Cuvellier M, Bruyère A, Legagneux V, Langouët S, Baffet G. Generation of proliferating human adult hepatocytes using optimized 3D culture conditions. Sci Rep 2021;11(1):515.
[21] Hydbring P, Malumbres M, Sicinski P. Non-canonical functions of cell cycle cyclins and cyclin-dependent kinases. Nat Rev Mol Cell Biol 2016;17(5):280–292.

[22] Braun LJ, Stegmeyer RI, Schäfer K, Volkery S, Currie SM, Kempe B, Nottebaum AF, Vestweber D. Platelets docking to VWF prevent leaks during leukocyte extravasation by stimulating Tie-2. Blood 2020;136(5):627–639.

[23] Morishita T, Hayakawa F, Sugimoto K, Iwase M, Yamamoto H, Hirano D, Kojima Y, Imoto N, Naoe T, Kiyoi H. The photosensitizer verteporfin has light-independent anti-leukemic activity for Ph-positive acute lymphoblastic leukemia and synergistically works with dasatinib. Oncotarget 2016;7(35):56241–56252.

[24] **Sorrentino G**, **Rezakhani S**, Yildiz E, Nuciforo S, Heim MH, Lutolf MP, Schoonjans K. Mechano-modulatory synthetic niches for liver organoid derivation. Nat Commun 2020;11(1):3416.

[25] Kudo N, Matsumori N, Taoka H, Fujiwara D, Schreiner EP, Wolff B, Yoshida M, Horinouchi S. Leptomycin B inactivates CRM1/exportin 1 by covalent modification at a cysteine residue in the central conserved region. Proc Natl Acad Sci U S A 1999;96(16):9112–9117.

[26] Apte U, Gkretsi V, Bowen WC, Mars WM, Luo JH, Donthamsetty S, Orr A, Monga SP, Wu C, Michalopoulos GK. Enhanced liver regeneration following changes induced by hepatocyte-specific genetic ablation of integrin-linked kinase. Hepatology 2009;50(3):844–851.

[27] Panciera T, Azzolin L, Cordenonsi M, Piccolo S. Mechanobiology of YAP and TAZ in physiology and disease. Nat Rev Mol Cell Biol 2017;18(12):758–770.

[28] Michalopoulos GK, DeFrances MC. Liver regeneration. Science 1997;276(5309):60–66.

[29] **Chembazhi UV**, **Bangru S**, Hernaez M, Kalsotra A. Cellular plasticity balances the metabolic and proliferation dynamics of a regenerating liver. Genome Res 2021;31(4):576–591.

[30] Yagi S, Hirata M, Miyachi Y, Uemoto S. Liver regeneration after hepatectomy and partial liver transplantation. Int J Mol Sci 2020;21(21):8414.

[31] **Poisson J**, **Lemoinne S**, Boulanger C, Durand F, Moreau R, Valla D, Rautou PE. Liver sinusoidal endothelial cells: physiology and role in liver diseases. J Hepatol 2017;66(1):212–227.

[32] Wake K. Hepatic stellate cells: three-dimensional structure, localization, heterogeneity and development. Proc Jpn Acad Ser B 2006;82(4):155–164.

[33] **Liu L**, **You Z**, Yu H, Zhou L, Zhao H, Yan X, Li D, Wang B, Zhu L, Xu Y, Xia T, Shi Y, Huang C, Hou W, Du Y. Mechanotransduction-modulated fibrotic microniches reveal the contribution of angiogenesis in liver fibrosis. Nat Mater 2017;16(12):1252–1261.

[34] Rohn F, Kordes C, Buschmann T, Reichert D, Wammers M, Poschmann G, Stuehler K, Benk AS, Geiger F, Spatz JP, Haeussinger D. Impaired integrin alpha(5)/beta(1)-mediated hepatocyte growth factor release by stellate cells of the aged liver. Aging Cell 2020;19(4):e13131.

[35] Zhang XK, Gauthier T, Burczynski FJ, Wang GQ, Gong YW, Minuk GY. Changes in liver membrane potentials after partial hepatectomy in rats. Hepatology 1996;23(3):549–551.

[36] Stacey DW. Cyclin D1 serves as a cell cycle regulatory switch in actively proliferating cells. Curr Opin Cell Biol 2003;15(2):158–163.

[37] Ledda-Columbano GM, Pibiri M, Loi R, Perra A, Shinozuka H, Columbano A. Early increase in cyclin-D1 expression and accelerated entry of mouse hepatocytes into S phase after administration of the mitogen 1, 4-Bis[2-(3,5-Dichloropyridyloxy)] benzene. Am J Pathol 2000;156(1):91–97.

[38] Michalopoulos GK. Advances in liver regeneration. Expert Rev Gastroenterol Hepatol 2014;8(8):897–907.

[39] Nishii K, Brodin E, Renshaw T, Weesner R, Moran E, Soker S, Sparks JL. Shear stress upregulates regeneration-related immediate early genes in liver progenitors in 3D ECM-like microenvironments. J Cell Physiol 2018;233(5):4272–4281.

[40] **Li N**, **Zhang X**, Zhou J, Li W, Shu X, Wu Y, Long M. Multiscale biomechanics and mechanotransduction from liver fibrosis to cancer. Adv Drug Deliv Rev 2022;188:114448.

[41] **Baptista PM**, **Moran EC**, Vyas D, Ribeiro MH, Atala A, Sparks JL, Soker S. Fluid flow regulation of revascularization and cellular organization in a bioengineered liver platform. Tissue Eng C-Methods 2016;22(3):199–207.

[42] Pu W, Zhang H, Huang X, Tian X, He L, Wang Y, Zhang L, Liu Q, Li Y, Li Y, Zhao H, Liu K, Lu J, Zhou Y, Huang P, Nie Y, Yan Y, Hui L, Lui KO, Zhou B. Mfsd2a+ hepatocytes repopulate the liver during injury and regeneration. Nat Commun 2016;7:13369.

[43] Wei Y, Wang YG, Jia Y, Li L, Yoon J, Zhang S, Wang Z, Zhang Y, Zhu M, Sharma T, Lin YH, Hsieh MH, Albrecht JH, Le PT, Rosen CJ, Wang T, Zhu H. Liver homeostasis is maintained by midlobular zone 2 hepatocytes. Science 2021;371(6532):eabb1625.

[44] Komatsu H, Koo A, Guth PH. Leukocyte flow dynamics in the rat liver microcirculation. Microvasc Res 1990;40(1):1–13.

[45] Wisse E, De Zanger RB, Charels K, Van Der Smissen P, McCuskey RS. The liver sieve: considerations concerning the structure and function of endothelial fenestrae, the sinusoidal wall and the space of Disse. Hepatology 1985;5(4):683–692.

[46] Oliva-Vilarnau N, Vorrink SU, Ingelman-Sundberg M, Lauschke VM. A 3D cell culture model identifies Wnt/β-catenin mediated inhibition of p53 as a critical step during human hepatocyte regeneration. Adv Sci 2020;7(15):2000248.

[47] **Nakatsuka H**, **Sokabe T**, Yamamoto K, Sato Y, Hatakeyama K, Kamiya A, Ando J. Shear stress induces hepatocyte PAI-1 gene expression through cooperative Sp1/Ets-1 activation of transcription. Am J Physiol Gastrointest Liver Physiol 2006;291(1):G26–G34.

[48] Yu H, Shen Y, Jin J, Zhang Y, Feng T, Liu X. Fluid shear stress regulates HepG2 cell migration though time-dependent integrin signaling cascade. Cell Adh. Migr 2018;12(1):56–68.

[49] Liu QP, Luo Q, Deng B, Ju Y, Song GB. Stiffer matrix accelerates migration of hepatocellular carcinoma cells through enhanced aerobic glycolysis via the MAPK-YAP signaling. Cancers 2020;12(2):490.